



Research Article

Structural, Optical and Antibacterial Response of CaO Nanoparticles Synthesized via Direct Precipitation Technique

Suresh Kumar^{1,2}, Vandana Sharma¹, Jatindra Kumar Pradhan³, Sanjay Kumar Sharma⁴, Prem Singh⁵, Jatinder Kumar Sharma¹✉

¹Department of Physics, MMEC, Maharishi Markandeshwar (Deemed to be University), Mullana, 133207, Haryana, India.

²Department of Physics, Maharishi Markandeshwar University - Sadopur, Ambala, 134007, Haryana, India.

³Department of Zoology, Department of Zoology, Kalahandi University, Kalahandi, 766001, Odisha, India.

⁴School of ICT, Gautam Buddha University, Greater Noida, 201308, Uttar Pradesh, India.

⁵S.D. College, Ambala Cantt., 133001, Haryana, India.

✉ Corresponding authors. E-mail: sureshlakhanpal@gmail.com; sharmajk.69@gmail.com

Received: Dec. 14, 2020; **Accepted:** Mar. 2, 2021; **Published:** May 18, 2021

Citation: Suresh Kumar, Vandana Sharma, Jatindra Kumar Pradhan, Sanjay Kumar Sharma, Prem Singh, and Jatinder Kumar Sharma, Structural, Optical and Antibacterial Response of CaO Nanoparticles Synthesized via Direct Precipitation Technique. *Nano Biomed. Eng.*, 2021, 13(2): 172-178.

DOI: 10.5101/nbe.v13i2.p172-178.

Abstract

Calcium oxide (CaO) is a promising material that works as a glass constituent, catalyst, toxic-waste remediation, poisonous gas absorbent, industrial refractory element for metal smelting, paper bleaching, sulfur neutralization in sugar, cosmetics and drug delivery mediator. This work proposes the synthesis of CaO nanoparticles by direct precipitation technique using an aqueous solution of calcium chloride and sodium hydroxide precursors. The synthesized nanoparticles are characterized for the structure, morphology, chemical composition and optical behavior using Fourier transform infrared (FTIR) spectroscopy, X-ray diffraction (XRD), field effect scanning electron microscopy (FE-SEM), energy dispersive X-ray spectroscopy (EDS), and diffuse reflectance spectroscopy. The XRD results show that the CaO nanoparticles have been synthesized in a cubic crystalline structure with the average crystallite size of about 13 nm and display aggregated morphology of nanoclusters. The presence of distinct peaks in the FTIR and EDS spectra reveal that the nanoparticles are successfully formed from the chemical recipe of the precipitation process. The optical bandgap has been estimated from the Kubelka-Munk plot and found to be 3.48 eV. The antibacterial activity of CaO nanoparticles has been tested by the well diffusion technique and observed that it shows good antibacterial action against the gram-negative bacterial strains.

Keywords: CaO nanoparticles, FTIR, XRD, Optical properties, Antibacterial activity

Introduction

The materials research in the past few decades dedicated to the metal oxide semiconductors (MOS) because of their enormous applications in many fields including photocatalysts, sensors, photonics, agriculture, electronics, optoelectronics, magnetism, superconductivity, environmental remediation, energy

storage and conversation, biomedical materials, etc. [1-8]. MOS are generally distinguished by their wide band gap behavior (> 3.0 eV) and most of them are inexpensive, safe, chemically stable and earth-abundant. The emerging science of nanomaterials shows a new way of material expansion where size ranging from 1 nm – 100 nm exhibits unique physicochemical properties. Thus, the MOS

nanoparticles with excellent features are expected to be a good choice for futuristic multifunctional materials.

Calcium oxide (CaO), also known as quicklime, is a caustic, alkaline, whitish chemical and the oldest known material that is used since the medieval age. It is crystalline solid at room temperature having oxidation number +2 and belongs to II-VI group of the periodic table. It is formed by an array of cations (Ca^{2+} ions) and anions (O^{2-} ions) having strong ionic bonding between them. However, the presence of moisture and water content in CaO converts it into slaked lime i.e. $\text{Ca}(\text{OH})_2$ [9]. It exhibits semiconducting properties and remains chemically stable at very high temperatures [9]. It is widely used in various fields as an efficient agent for ceramic, catalyst, cosmetic, waste remediation, destructive adsorbent for toxic chemicals and exhaust gases, targeted drug delivery and refractory additive in the paints [9–11]. It is also used to remove SO_2 or other sulfur containing pollutants from the exhaust gases [12]. Recently, the ultrafine particles of CaO are used as bactericide and antibacterial agents for controlling the microorganisms and absorbent [8, 13–15]. The common human diseases like typhoid, diarrhea, cholera, intestinal infections, etc., are due to the infection from water born bacterial pathogens. The vast use of antibiotics builds up antibacterial resistant characteristics in the microorganisms that easily deny medical treatment. Hence, the search for safe and alternate antibacterial materials to fight infectious organisms creates research interest toward MOS nanoparticles.

Moreover, the controlled production of MOS nanoparticles is essential for effective and successful applications. It has been reported that solution based chemical methods has excellent tendency to control the size, shape, distribution and other properties of the end products [4]. CaO and $\text{Ca}(\text{OH})_2$ nanoparticles are reported to synthesized by sol-gel method, thermal decomposition, precipitation, hydrothermal, microwave-assisted method, etc., [3, 9, 11–19]. Among all these methods, direct precipitation is simple, cost-effective, reproductive and rapid technique for nanoparticles synthesis [20–22].

Therefore, in this work direct precipitation technique was used to synthesize CaO nanoparticles and characterize them using Fourier transform infrared (FTIR) spectroscopy, X-ray diffraction (XRD), field effect scanning electron microscopy (FE-SEM), energy dispersive X-ray spectroscopy (EDS) and diffuse reflectance spectroscopy for different

properties. Moreover, the antibacterial activity of these nanoparticles was also studied against two gram negative pathogen bacteria, Escherichia coli (E. coli) and Vibrio cholerae (V. cholerae). As per our knowledge, this is the first report that has focused on the antibacterial response of CaO nanoparticles on V. cholerae bacteria.

Experimental

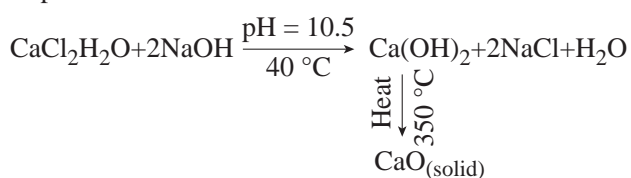
Chemicals

The analytical grade reagents calcium chloride anhydrous ($\text{CaCl}_2\text{H}_2\text{O}$) and sodium hydroxide (NaOH) of 99.9% purity were purchased from Merck (India) and used as received without any special treatment.

Sample preparation

In the present experiment, pure CaO nanoparticles are synthesized by direct precipitation method as it is one of the most versatile, cost effective, simple and conventional method for producing CaO and $\text{Ca}(\text{OH})_2$ in comparison to other synthesis methods. To synthesize CaO nanoparticles, 0.1 M solution CaCl_2 was prepared in 100 mL distilled water at 40 °C under continuous stirring for 1 h using hot plate magnetic stirrer. Then 50 mL solution of NaOH (0.1 M) prepared in distilled water was added dropwise into the CaCl_2 solution. The reaction process was carried out for 2 h at temperature 40 °C and pH = 10.5 which results in white color precipitates. These precipitates were sonicated, filtered and washed repeatedly with ethanol and distilled water which was further dried for 6 h at 60 °C. The end product of this chemical reaction was a precursor of CaO that is $\text{Ca}(\text{OH})_2$ which is finally calcinated at 350 °C for 2 h in a microwave oven. The obtained CaO nanoparticles kept in the vacuum desiccator before further characterization.

The synthesis of CaO nanoparticles by direct precipitation technique started with the initial precipitation of $\text{Ca}(\text{OH})_2$ during the chemical process from the dissolved Ca^{2+} and OH^- ions in the aqueous medium. As the concentration of these ions exceeds a critical value, precipitation of CaO nuclei starts under the calcination process to form solid CaO nanoparticles (Fig. 1). The chemical *reaction* process and synthesis steps as follows:



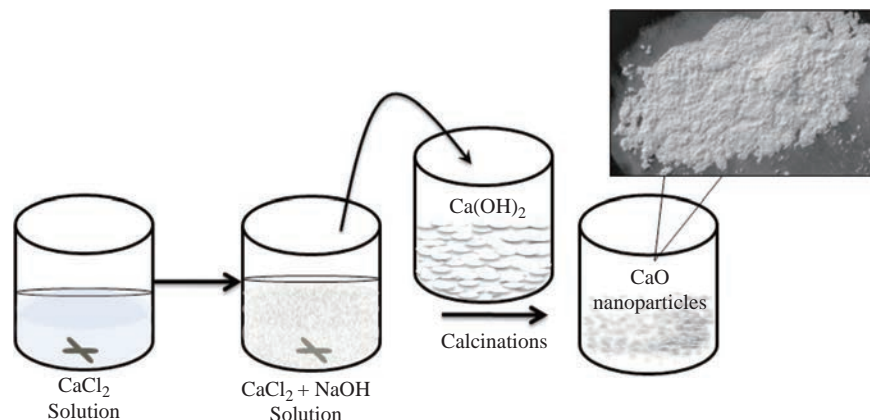


Fig. 1 Schematic illustration of the synthesis steps for CaO nanoparticles.

Characterization of CaO nanoparticles

The obtained CaO nanoparticles were subjected to physical analysis using Perkin Elmer 1600 Fourier transform infrared spectrometer with KBr pellet technique and PANalytical X'pert Pro X-ray diffractometer. The XRD pattern further matches with the standard JCPDS data cards. The morphology and elemental composition of nanoparticles were observed by Jeol JSM-6100 field emission scanning electron microscope equipped with energy dispersive X-ray analyzer. The optical study was carried out by Ultraviolet-visible (UV-vis) diffuse reflectance spectrometer (Schimadzu 2600) between the wavelength ranges of 200 to 800 nm.

Antibacterial activity test

Antibacterial activity test was performed against the gram-negative bacterial strains of *E. coli* and *V. cholerae* by agar well diffusion method. The stock cultures were prepared by inoculating the bacterial strains in Muller Hinton agar plates (Himedia, India) followed by the incubation at 37 °C for 24 h. These cultures were maintained at 4 °C until the preparation of the working cultures. The cultures were diluted with fresh Muller-Hinton broth to obtain optical densities of the order of 2.0×10^6 CFU/mL. Sterile pipettes were used for the transfer of 50 μ L molten agar to broth culture (0.5 mL) of test organisms, mixed properly and transferred into sterile dishes. The wells were prepared using sterile cork borer (6 mm) and each well was filled with different concentrations (5 mg/mL to 25 mg/mL) of CaO nanoparticles. The plates were incubated at 37 °C for 24 h. After incubation, the dishes were examined for the zone of inhibition and measured in terms of millimetre of the diameter.

Results and discussion

FTIR characterization of CaO nanoparticles

FTIR spectrum of CaO particles is shown in Fig. 2. The strong peak at 3642 cm^{-1} is assigned to the O–H free hydroxyl bond from the residual hydroxide or the moisture content in the sample [9]. This peak is sharp well which indicates the formation of pure phase particles. The residual hydroxyl groups further supported by the presence of absorbance bands in the region of $\sim 1600 \text{ cm}^{-1}$ and $\sim 800 \text{ cm}^{-1}$ [9, 22]. The strong broad band at 1471 cm^{-1} and a peak at 876 cm^{-1} indicate the C–O bond arose because of the carbonation of CaO nanoparticles [9]. During calcination, the exposure of highly reactive surface area of CaO nanoparticles to air during leads to CO_2 and H_2O formation which further adsorbed on the CaO surface in the form of free –OH and carbonate species. This specifies that the surface –OH and the lattice oxygen of CaO nanoparticles make available oxygen which is more liable on the high surface area of the nanoparticles [16]. Two small dips at in the spectra at 1229 cm^{-1} , 1633 cm^{-1} and 2515 cm^{-1} attributed to C–

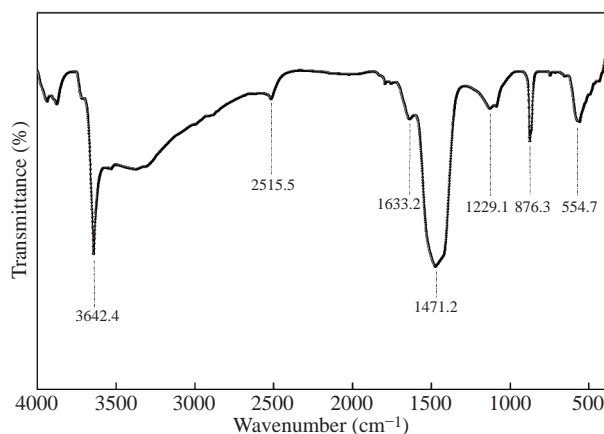


Fig. 2 FTIR spectrum of CaO nanoparticles.

O stretch of the CO₂ stretching [17]. The characteristic peak at 554 cm⁻¹ has been detected for Ca–O bond stretch. Hence, we can say that FTIR analysis justifies the traces of chemicals used in the synthesis of CaO nanoparticles.

XRD characterization of CaO nanoparticles

Fig. 3 shows the XRD spectrum for the synthesized CaO nanoparticles which is measured over the diffraction angle (2θ) between 20° to 80° using Cu(K α) source. The presence of highly intense and multiple XRD peaks with broadening nature indicate that the product is well crystallized. On comparing with the standard diffraction pattern (Table 1), five distinguish peaks (\ominus) indexed to the cubic (zinc blende) structure (space group Fm3m, JCPDS card No. 82–1690) for CaO nanoparticles [23]. These diffraction peaks at position $2\theta = 32.1^\circ, 37.5^\circ, 54.2^\circ, 65.7^\circ$ and 67.5° belong to (111), (200), (202), (311), and (222) reflection planes respectively. Further, two additional peaks (Δ) at $2\theta = 50.5^\circ$ and 57.7° are also observed that match with (110) and (003) planes of Ca(OH)₂ with hexagonal structure (Portlandite, JCPDS card No. 04–0733) [9]. The existence of these impure phase peaks of Ca(OH)₂ may be due to the presence of moisture content in the synthesized nanoparticles. This moisture content appears as a result of solution-based synthesis of nanoparticles and their exposure to the environment after synthesis that results to the oxidation of CaO. The interplanar spacing (d-spacing) between different crystal planes of cubic the CaO structure is calculated using Bragg diffraction equation and represented in Table 1.

The crystallite size (D) has been calculated for all peaks (Table 1) using Debye–Scherrer’s formula [21]: $D = (k\lambda)/(\beta\cos\theta)$

where k , λ , β and θ are the shape factor (0.81), X-ray wavelength (1.5406 Å), full width at half maximum and Bragg diffraction angle respectively. The average crystallite size is found to be 13.5 nm.

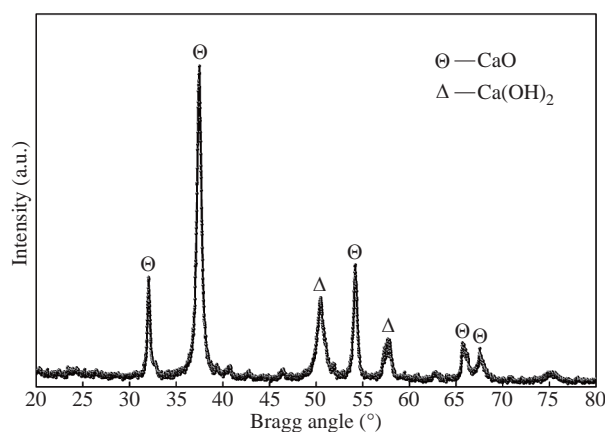


Fig. 3 XRD spectrum of CaO nanoparticles.

Many researchers have been reported different size CaO nanoparticles by different solution methods. Mirghiasi Z, et. al have synthesized CaO and Ca(OH)₂ nanoparticles having crystallite size of 40 nm and 41 nm respectively via direct decomposition method [9]. Habte et al. have reported sol-gel synthesized CaO nanoparticles of size 24.51 nm from waste eggshell [18]. Roy et al. synthesized cubic CaO nanoparticles of size 16 nm by microwave irradiation method. However, the present study successfully attains the smallest size CaO nanoparticles [13]. The lattice constant ($a = d\sqrt{h^2 + k^2 + l^2}$) for cubic CaO nanoparticles is calculated from the most intense XRD peak and found to be 4.793 nm. The small variation in the value of lattice constant and d-spacing from that of the bulk value is attributed to the presence of microstrain and defects that occurred during the growth process. These microstrain and dislocation densities have been determined (Table 1) using the relation given by Dhupar et al. [22] with an average value of 2.764×10^{-3} and 6.32×10^{-15} line/m² respectively.

FE-SEM characterization of CaO nanoparticles

Fig. 4(a)-(c) shows the surface morphology of the synthesized nanoparticles at three different magnification scales (1 μ m, 500 nm and 200 nm). The

Table 1 Structural properties of CaO nanoparticles analyzed from XRD spectrum and values from standard JCPDS data card No. 82–1690

2 θ (°)		d-spacing (Å)		Intensity (I/I ₀)	β (°)	Particle size (nm)	(hkl)	Micro stain ($\times 10^{-3}$)	Dislocation density ($\times 10^{15}$) line/m ²
Observed	JCPDS	Observed	JCPDS						
32.10	32.20	2.786	2.779	34	0.4909	17.6	(111)	4.14	3.23
37.50	37.35	2.396	2.407	100	0.6949	12.6	(200)	3.25	6.29
54.20	53.85	1.691	1.702	38	0.5679	16.4	(311)	3.30	3.71
65.70	64.15	1.420	1.451	14	0.9151	10.8	(220)	1.41	8.58
67.50	67.37	1.387	1.390	12	0.9857	10.1	(222)	1.72	9.79

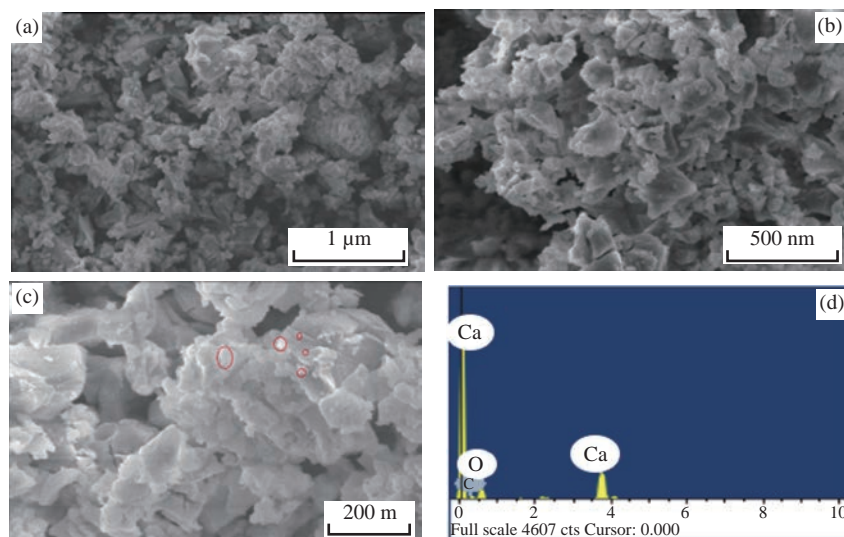


Fig. 4 FE-SEM micrographs at magnification scales (a) 1 μm , (b) 500 nm and (c) 200 nm, and EDS spectra of CaO nanoparticles.

grown particles are observed to be closely packed in the cluster cum porous arrangements which makes them more active in the catalysis and gas sorbent applications. These particles appeared to be solid, fully developed and randomly scattered with non-uniform cubical dimensions. The size of individual CaO nanoparticles, which are available freely on the surface, has been calculated using inception method (Fig. 4(c)) and found to vary from 20 nm to 80 nm. The EDS spectrum (Fig. 4(d)) of CaO nanoparticles indicates that the Ca and O elements are present in the sample while the peak of carbon arises due to the coating used in the analysis. The atomic ratio of Ca and O is found to be 48.85:51.15 which is inconsistent with the stoichiometry of CaO and slightly rich in oxygen content.

Optical characterization of CaO nanoparticles

UV-vis diffuse reflectance spectra in absorbance mode of the CaO nanoparticles has been recorded for the wavelength of 200 nm to 800 nm (inset of Fig. 5). It is obvious that the absorption edge observed at 360 nm i.e., in the UV-light region and almost negligible absorption in the visible region.

The optical band gap of CaO nanoparticles (Fig. 5) was calculated by plotting $F(R)^2$ vs. photon energy (hv) from the Kubelka-Munk function $F(R)$ [20] which is related to the diffuse reflectance (R) as $F(R) = (1-R)^2/2R$.

The linear part of this curve is extrapolated to zero on the energy axis to get the value of optical band gap. The value of optical band gap thus obtained to be 3.48 eV which is lower than the value (6.26 eV) for bulk

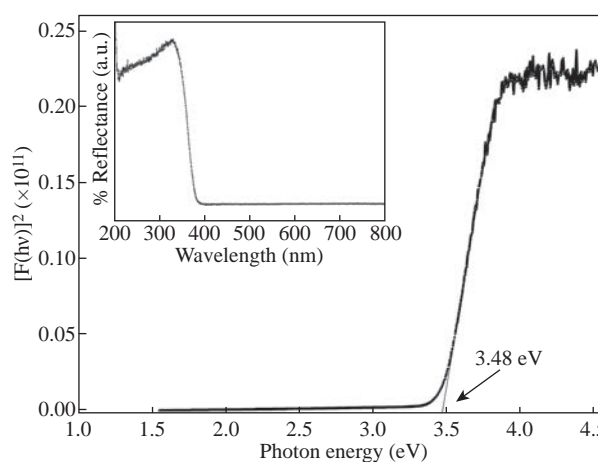


Fig. 5 The estimation of optical band gap by Kubelka-Munk plot of $F(R)^2$ vs. $h\nu$ and the inset shows UV-vis diffuse reflectance spectra of CaO nanoparticles.

CaO but found compatible with the reported results for CaO nanoparticles by different researches [11, 19]. This low value of optical band gap may be associated with the presence of $\text{Ca}(\text{OH})_2$ phase in the CaO nanoparticles which provides defect states between the energy gap and reduces the band gap.

Antibacterial Activity of CaO nanoparticles

The antibacterial activities of CaO nanoparticles, at different concentrations of 5, 10, 15, 20 and 25 mg/mL, against both bacterial strains (*E. coli* and *V. cholera*), have been shown in Fig. 6. It clearly demonstrates that the antibacterial activity of the CaO nanoparticles could be effective against the pathogenic bacteria by increasing the concentration of nanoparticles. The antibacterial results have indicated that the degree of the zone of inhibition is more against bacterial strain *E. coli* (28 ± 0.15 mm) when compared to the

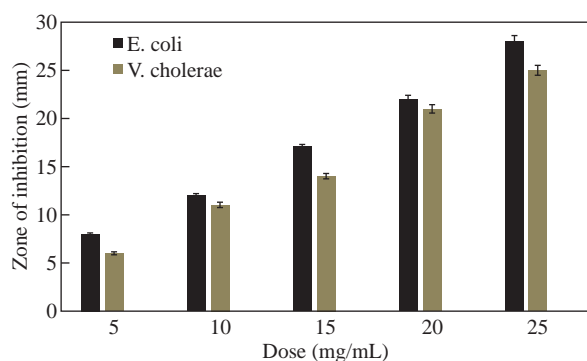


Fig. 6 Antibacterial activity of CaO nanoparticles against *E. coli* and *V. cholerae*.

V. cholerae (25 ± 0.10 mm) at all concentrations of nanoparticles. The trend of antibacterial activity of the CaO nanoparticles for these gram-negative bacteria is almost the same, which agrees well with the previous reports [15, 23]. The creation of an inhibition zone evidently states the mechanism of the biocidal properties of nanoparticles that lead to the disruption of the bacterial membrane [23]. Since nanoparticles exhibit large surface area so they can tightly attach to the surface of the bacterial cells and penetrate easily into the membrane [24]. This would result in the leakage of intracellular components of the cell that kills the bacterial cell. The range of inhibition depends on the concentration of nanoparticles and increases with the increase in concentration.

Conclusions

In conclusion, we have successfully synthesized CaO nanoparticles by direct precipitation technique at the optimized value of temperature (40 °C) and pH (10.5) within a period of 2 h. The synthesized nanoparticles are characterized for different features using FTIR, XRD, FE-SEM, EDS and diffuse reflectance spectroscopy. FTIR analysis evidenced the presence of prime O–H and Ca–O stretching modes around 3642 cm^{-1} and 554 cm^{-1} respectively, attributed to the presence of the desired phase which is confirmed by XRD results. XRD investigation revealed the existence of cubic zinc blende structure of CaO nanoparticles of size 13.5 nm along with some content of hexagonal Ca(OH)_2 as a separate phase. FE-SEM micrographs exposed the presence of agglomerated cubical nanoparticles. The peaks in the EDX spectra representing Ca and O elements only are demonstrating the successful formation of CaO nanoparticles. A low optical bandgap value of 3.48 eV for CaO nanoparticles is associated with the

existence of Ca(OH)_2 phase. The synthesized cubical CaO nanoparticles showed good antibacterial activity against gram-negative bacteria strains of *E. coli* and *V. cholera*, which is well demonstrated by the well diffusion method. The synthesized CaO nanoparticles having unique structural, optical and antibacterial response can be exploited in near future for eco-friendly agents for many biomedical applications and targeted drug delivery systems.

Acknowledgments

We are very much thankful to SAIF, Chandigarh and Maharishi Markandeshwar (Deemed to be University) - Mullana for various instrumentation and test facilities.

Conflict of Interests

The authors declare that no competing interest exists.

References

- [1] J. Hao, N.X. Sun, J. Qiu et al., Structural, electronic and optical properties of functional metal oxides. *Advances in Condensed Matter Physics*, 2014: Article ID 134951, 1-2.
- [2] X. Yu, T.J. Marks, and A. Facchetti, Metal oxides for optoelectronic applications. *Nature Materials*, 2016, 15: 383-396.
- [3] J. Suresh, G. Pradheesh, V. Alexramani, et al., Green synthesis and characterization of zinc oxide nanoparticle using insulin plant (*Costus pictus* D. Don) and investigation of its antimicrobial as well as anticancer activities. *Advances in Natural Sciences: Nanoscience and Nanotechnology*, 2018, 9: 015008.
- [4] A.V. Nikam, B.L.V. Prasad, and A.A. Kulkarni, Wet chemical synthesis of metal oxide nanoparticles: A review. *CrystEngComm*, 2018, 20: 5091-5107.
- [5] M.S. Chavali, M.P. Nikolova, Review paper metal oxide nanoparticles and their applications in nanotechnology. *SN Applied Sciences*, 2019, 1: 607, 1-30.
- [6] P. Riente, T. Noel, Application of metal oxide semiconductors in light-driven organic transformation. *Catalysis Science & Technology*, 2019, 9: 5186-5232.
- [7] Y.S. Rim, Review of metal oxide semiconductors-based thin-film transistors for point-of-care sensor applications. *Journal of the Society for Information Display*, 2020, 7: 1-8.
- [8] Y.A. Ali, A. Hilal, P. Tabassum, et al., Recent advances in metal decorated nanomaterials and their various biological applications: A review. *Frontiers in Chemistry*, 2020, 8(341): 1-23.
- [9] Z. Mirghiasi, F. Bakhtiari, E. Darezereshki, et al., Preparation and characterization of CaO nanoparticles from Ca(OH)_2 by direct thermal decomposition method. *Journal of Industrial and Engineering Chemistry*, 2014, 20: 113-117.
- [10] M.A. Alavi, A. Morsali, Ultrasonic-assisted synthesis of Ca(OH)_2 and CaO nanostructures. *Journal of Experimental Nanoscience*, 2010, 5: 93-105.

- [11] A.R. Butt, S. Ejaz, J.C. Baron, et al., CaO nanoparticles as a potential drug delivery agent for biomedical applications. *Digest Journal of Nanomaterials and Biostructures*, 2015, 10: 799-809.
- [12] X. Shao, P. Myrach, N. Nilius et al., Growth and morphology of calcium-oxide films grown on Mo(001). *The Journal of Physical Chemistry C* 2011, 115: 8784-8789.
- [13] A. Roy, S.S. Gauri, M. Bhattacharya et al., Antimicrobial activity of CaO nanoparticles. *Journal of Biomedical Nanotechnology*, 2013, 9: 1570-1578.
- [14] M. Ramli, R.B. Rossani, Y. Nadia, et al., Nanoparticle fabrication of calcium oxide (CaO) mediated by the extract of red dragon fruit peels (*Hylocereus Polyrhizus*) and its application as inorganic-anti-microorganism materials. *IOP Conference Series: Materials Science and Engineering*, 2019, 509: 012090
- [15] G. Marquis, B. Ramasamy, S. Banwarilal, et al. Evaluation of antibacterial activity of plant mediated CaO nanoparticles using *cissus quadrangularis* extract. *The Journal of Photochemistry and Photobiology B*, 2016, 155: 28-33.
- [16] A. Imtiaz, M.A. Farrukh, M. Khaleeq-ur-Rahman, et al., Micelle-assisted synthesis of $Al_2O_3 \cdot CaO$ nanocatalyst: optical properties and their applications in photodegradation of 2,4,6-trinitrophenol. *The Scientific World Journal*, 2013: Article ID 641420, 1-11.
- [17] A. Samanta, D.K. Chanda, P.S. Das, et al., Synthesis of nano calcium hydroxide in aqueous medium. *Journal of the American Ceramic Society*, 2016, 99: 787-795.
- [18] L. Habte, N. Shiferaw, D. Mulatu, et al., Synthesis of nano-calcium oxide from waste eggshell by sol-gel method. *Sustainability*, 2019, 11: 3196, 1-10.
- [19] N. Lalou, A. Kadari, Influence of Li^{2+} doping on the structural and optical properties of CaO synthesized by sol-gel process. *Journal of Molecular and Engineering Materials*, 2019, 7: 1950002, 1-5.
- [20] S. Kumar, D. Arora, A. Dhupar, et al., Structural and optical properties of polycrystalline ZnO nanopowder synthesized by direct precipitation technique. *Journal of Nano-Electronic Physics*, 2020, 12: 04027-5.
- [21] S. Kumar, J.K. Sharma, Stable phase CdS nanoparticles for optoelectronics: a study on surface morphology, structural and optical characterization. *Materials Science Poland*, 2016, 34: 368-373.
- [22] A. Dhupar, S. Kumar, V. Sharma, et al., Mixed structure Zn(S,O) nanoparticles: Synthesis and characterization. *Materials Science Poland*, 2019, 37: 230-237.
- [23] G. Gedda, S. Pandey, Y.C. Lin, et al., Antibacterial effect of calcium oxide nano-plates fabricated from shrimp shells. *Green Chemistry*, 2015, 17: 3276-3280.
- [24] N. Yazdani, J. Javadpour, B.E. Yekta, et al., Hydrothermal synthesis of cobalt-doped hydroxyapatite nanoparticles: structure, magnetic behaviour, bioactivity and antibacterial activity. *Iranian Journal of Materials Science and Engineering*, 2019, 16: 39-48.

Copyright© Suresh Kumar, Vandana Sharma, Jatindra Kumar Pradhan, Sanjay Kumar Sharma, Prem Singh, and Jatinder Kumar Sharma. This is an open-access article distributed under the terms of the Creative Commons Attribution License, which permits unrestricted use, distribution, and reproduction in any medium, provided the original author and source are credited.